Proc. Natl. Acad. Sci. USA
Vol. 95, pp. 6630–6635, June 1998
Biochemistry

Structural basis for chemical inhibition of human blood coagulation factor Xa

KENJI KAMATA*†, HIROSHI KAWAMOTO†, TERUKI HONMA†, TOSHIHARU IWAMA†, AND SUNG-HOU KIM*‡

*Department of Chemistry and Lawrence Berkeley National Laboratory, University of California, Berkeley, CA 94720-5230; and †Tsukuba Research Institute, Banyu Pharmaceutical Co., Ltd., Okubo 3 Tsukuba 300–33, Japan

Contributed by Sung-Hou Kim, March 18, 1998

ABSTRACT **Factor Xa, the converting enzyme of prothrombin to thrombin, has emerged as an alternative (to thrombin) target for drug discovery for thromboembolic diseases. An inhibitor has been synthesized and the crystal structure of the complex between Des[1–44] factor Xa and the inhibitor has been determined by crystallographic methods in two different crystal forms to 2.3- and 2.4-Å resolution. The racemic mixture of inhibitor FX-2212, (2*RS*)-(3′-amidino-3-biphenylyl)-5-(4-pyridylamino)pentanoic acid, inhibits factor Xa activity by 50% at 272 nM *in vitro*. The *S*-isomer of FX-2212 (FX-2212a) was found to bind to the active site of factor Xa in both crystal forms. The biphenylamidine of FX-2212a occupies the S1-pocket, and the pyridine ring makes hydrophobic interactions with the factor Xa aryl-binding site. Several water molecules meditate inhibitor binding to residues in the active site. In contrast to the earlier crystal structures of factor Xa, such as those of apo-Des[1–45] factor Xa and Des[1–44] factor Xa in complex with a naphthyl inhibitor DX-9065a, two epidermal growth factor-like domains of factor Xa are well ordered in both our crystal forms as well as the region between the two domains, which recently was found to be the binding site of the effector cell protease receptor-1. This structure provides a basis for designing next generation inhibitors of factor Xa.**

Thromboembolic disease is caused by the improper functioning of the blood coagulation process. Blood clots are formed by a zymogen activation cascade of serine proteases, and the last protease of the cascade, thrombin, converts fibrinogen to fibrin, which cross-links to form blood clots (for a review, see ref. 1). To find antithrombotic drugs, many inhibitors of thrombin have been developed (2–5). But factor Xa, which is also essential for both the intrinsic and extrinsic pathways of the coagulation process, is thought to be a better target of antithrombotic drugs because many thrombin inhibitors have been shown to increase the risk of abnormal bleeding (6–8).

Factor X is secreted into the blood as the zymogen form of the serine protease and is converted to an active form, factor Xa, by the factor VIIa/tissue factor complex (in the extrinsic pathway) or by the factor IXa/factor VIIIa complex (in the intrinsic pathway) (1). Both complexes remove the activation peptide of factor X by limited proteolytic cleavage to form mature factor Xa. Factor Xa leads to blood clot formation by converting prothrombin to thrombin. In the presence of Ca^{2+} ions, factor Xa forms prothrombinase with factor Va on the phospholipid membrane of the activated platelets.

Furthermore, the binding of factor Xa to effector cell protease receptor-1 (EPR-1) participates in the activation of lymphocytes (9, 10) and arterial smooth muscle cells (11). Recent research also suggests that EPR-1 is required for the prothrombinase formation on the platelet membranes (12).

Factor Xa consists of a light chain and a heavy chain linked by a single disulfide bond. The light chain contains the N-terminal Gla domain and two epidermal growth factor (EGF)-like domains. The Gla domain contains 11 γ-carboxyglutamic acid residues and mediates binding to the negatively charged phospholipid membrane in the presence of Ca^{2+} ions. The role of the EGF domains are not clear yet, but recent research suggests that the region between the two EGF domains is the binding site of EPR-1 (13, 14). The heavy chain contains a trypsin-like serine protease domain. This domain organization is very similar to those of other blood coagulation enzymes such as factor VIIa, factor IXa, and protein C (1).

The crystal structure of human factor Xa has been determined in apo form (15) and as a complex with the inhibitor DX-9065a, (2*S*)-{4-[1-acetimidoyl-(3*S*)-pyrrolidinyl]oxyphenyl}-3-(7-amidino-2-naphthyl)propionic acid (Fig. 1; ref. 16). But in both structures, the first EGF domain and the region between the two EGF domains were disordered. In contrast, these regions are well ordered in our crystal structure of the complex between Des[1–44] factor Xa and FX-2212a (Fig. 1), a new inhibitor with an IC_{50} of 272 nM and an apparent K_i of 131 nM (measured for the racemic mixture of FX-2212). This inhibitor was synthesized as an initial lead for structure-based inhibitor design for factor Xa. Our structure reveals the details of the binding mode of the *S*-isomer of FX-2212, FX-2212a, as well as the structures of two, hitherto unknown regions: the first EGF domain and the binding site of EPR-1.

METHODS

Human factor Xa β-form was purchased from Haematologic Technologies, (Burlington, VT) and converted to Des[1–44] factor Xa by chymotrypsin digestion (17, 18), thus removing the Gla domain. FX-2212 was synthesized as outlined in Fig. 2. The inhibitor was confirmed by ^{1}H-NMR spectra on a Varian VXR 300 (300 MHz) spectrometer and high resolution mass spectra on a JEOL JMS-SX102A spectrometer. FX-2212 is one of the strongest inhibitors among ≈200 initial lead compounds we have synthesized. Inhibition assays of factor Xa and thrombin were measured by using S-2765 (Chromogenix, Molndal, Sweden) as a substrate in a solution of 20 mM Hepes (pH 7.4), 150 mM NaCl, and 2 mM $CaCl_2$ at various inhibitor concentrations. IC_{50} was determined at 0.2 mM S-2765. To

The publication costs of this article were defrayed in part by page charge payment. This article must therefore be hereby marked "*advertisement*" in accordance with 18 U.S.C. §1734 solely to indicate this fact.

Abbreviations: FX-2212, (2*RS*)-(3′-amidino-3-biphenylyl)-5-(4-pyridylamino)pentanoic acid; FX-2212a, (2*S*)-(3′-amidino-3-biphenylyl)-5-(4-pyridylamino)pentanoic acid; DX-9065a, (2*S*)-{4-[1-acetimidoyl-(3*S*)-pyrrolidinyl]oxyphenyl}-3-(7-amidino-2-naphthyl) propionic acid; EPR-1, effector cell protease receptor-1; EGF, epidermal growth factor; Gla, γ-carboxyglutamic acid.

Data deposition: The atomic coordinates have been deposited in the Protein Data Bank, Biology Department, Brookhaven National Lab-

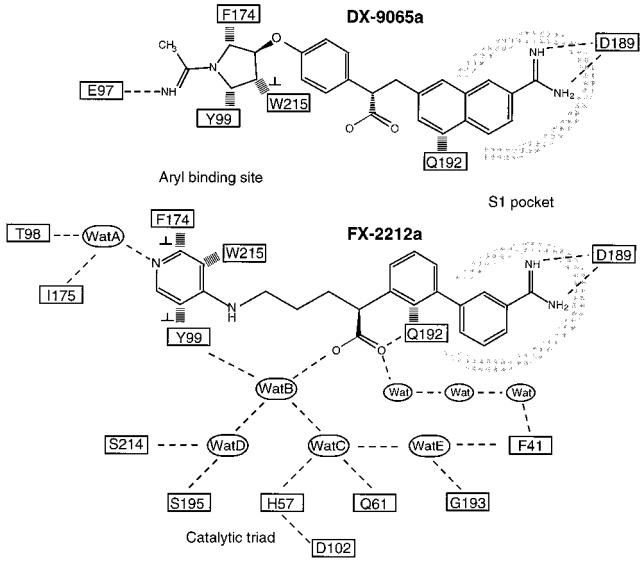

FIG. 1. Chemical formulae of the FX-2212a inhibitor (2*S*)-(3′-amidino-3-biphenylyl)-5-(4-pyridylamino)pentanoic acid and the DX9065a (2*S*)-{4-[1-acetimidoyl-(3*S*)-pyrrolidinyl]oxyphenyl}-3-(7-amidino-2-naphthyl)propionic acid. Schematic drawing of the interactions between two inhibitors, DX9065a and FX-2212a, and factor Xa. Hydrogen bonds are shown as thin dashed lines, and hydrophobic interactions are shown as thick dashed lines. In the case of Q192, the aliphatic chain portion of Q192 makes the hydrophobic interaction. The symbol "⊥" indicates that the two interacting aromatic groups are not stacked but are perpendicular to each other.

determine the K_i value, inhibition assays were performed at different substrate concentrations ranging from 0.0 to 0.4 mM.

Des[1–44] factor Xa in complex with FX-2212 was crystallized into two different crystal forms. The crystallization conditions were found by sparse matrix methods (19) by using Crystal Screens (Hampton Research, Riverside, CA) and were optimized. Form 1 crystals were obtained from a solution containing 5 mg/ml Des[1–44] factor Xa, 1 mM FX-2212, 10% polyethylene glycol 3350, 50 mM Mes pH 6.0, 100 mM Li_2SO_4, and 4 mM $CaCl_2$ by vapor phase equilibration. The crystals appeared within 1 month. Form 2 crystals were obtained from a solution containing 5 mg/ml Des[1–44] factor Xa, 1 mM FX-2212, 10% polyethylene glycol 3350, 50 mM malate–imidazole (pH 5.5), 250 mM sodium acetate, and 4 mM $CaCl_2$ also by vapor phase equilibration. This crystal form appeared within 1 week. Form 1 crystals belonged to space group $P2_1$ (a = 58.3 Å, b = 105.2 Å, c = 63.2 Å, β = 103.4°) with two molecules per asymmetric unit, and form 2 crystals belonged to space group $P2_12_12_1$ (a = 61.5 Å, b = 65.8 Å, c = 81.4 Å) with one molecule in an asymmetric unit. X-ray diffraction data from a form 1 crystal to 2.4-Å resolution were collected on an R-axis IIc area detector (Rigaku Co., Tokyo), and data from a form 2 crystal were collected to 2.3-Å resolution at the X12B beam line at the Brookhaven National Laboratory. Both data sets were collected under flash freezing conditions (100 K) by using 15% glycerol and 7.5% 2,3-butanediol as a cryoprotectant, respectively. The data reduction statistics from the DENZO and the SCALEPACK (20) processing are given in Table 1.

The structures were solved by the molecular replacement method by using the AMORE program (21, 22) with the data of a resolution from 15.0 to 3.5 Å. The human Des[1–45] factor Xa structure (ref. 15; Protein Data Bank Identification: 1HCG) was used as the search model. The two best and the next best solutions of the rotation search had the signals ≈15 times and 5 times higher than the background, respectively, for search were >9 times and 2.5 times for the form 1 crystal and 18 times and 9 times for the form 2 crystal, respectively. After rigid body refinement, the *R*-factors were 38.9% and 42.5% for the form 1 and 2 crystals, respectively. After building the first EGF domain model and a few refinement cycles, the electron density for the inhibitor was found in a difference density map (see Fig. 5*a*). Model building, electron density map calculation, and model refinement were performed with the X-PLOR (23–25) and the O (26) programs. The crystal structure in the form 1 crystal was refined to an *R* value of 20.6% (*R* free = 29.4%), and that in the form 2 crystal was refined to an *R* value of 19.6% (*R* free = 28.7%) with good stereochemistry (Table 1).

RESULTS

Overall Structure of Factor Xa. The crystal structure of Des[1–44] factor Xa (Fig. 3) has an elongated shape similar to those of protein C (27), factor VIIa (28), and factor IXa (29) except for the Gla domain, which was removed. Although the first EGF domain was disordered in both structures of apo (15) and DX-9065a-bound factor Xa (16), electron density for this domain was unambiguous in both forms 1 and 2 crystals. The structures of the second EGF domain and the catalytic domain have the same structure as those of the apo factor Xa structure (18) for the most part. Between our structures and the apo factor Xa structure, rms differences in the Cα positions of the catalytic domains average 0.41 Å for the form 1 crystal and 0.43 Å for the form 2 crystal. The small structural differences were caused by the inhibitor FX-2212 and calcium binding, as well as by the presence of an autolysis loop in our structures. The autolysis loop [Arg-143–Arg-154 using the chymotrypsin numbering system (15)], which was cleaved off of the apo factor Xa crystals (15), clearly was ordered in both form 1 and 2 crystals. The catalytic domain has one bound calcium in both crystal forms. The presence of the autolysis loop and the calcium binding induced only small structural changes.

The folding of the first EGF domain is similar to that of factor IXa (29) and bovine factor X (30–32). The domain has one calcium binding site as in factor VII and factor IX. Among three molecules in our two crystal forms, we found only one poorly ordered Ca^{2+} ion in this site despite the presence of 4 mM $CaCl_2$ in the crystallization solutions. The lack of the Gla domain might have destabilized the structure of the calcium binding site and decreased the affinity for calcium. The ligands for Ca^{2+} are Oε of Gln-L49, Oδ of Hya (β-hydroxyaspartic acid) L63, O of Leu-L65, and O of Gly-L64; the prefix "L" is for the light chain.

Binding Site of EPR-1. Recent studies suggest that the region (Leu-L83–Leu-L88) between the two EGF domains of factor Xa is the binding site for EPR-1 (13, 14). The structure of this region was not visible in either the apo (15) or DX-9065a-bound factor Xa (16) structure because of disorder. In both form 1 and 2 crystals, the region appears as a extended segment (Fig. 3). Although both EGF domains have very similar structures to those of factor IXa (29), the relative arrangement of these two domains is very different because of the different lengths and structures of the inter-EGF domain region. This difference is also true among the three crystallographically independent molecules in our two crystal forms (Fig. 4). In all three molecules, there is no interaction between the first and the second EGF domains, in contrast to the ball-and-socket-like interaction in factor IXa (29). Because a hexa-peptide of the sequence Leu-Phe-Thr-Arg-Lys-Leu, which is present in the region between the two EGF domains, recapitulates the inflammatory response, this extended structure is thought to be required for recognition by EPR-1 (13). EPR-1 may contribute to the complex formation of prothrom-

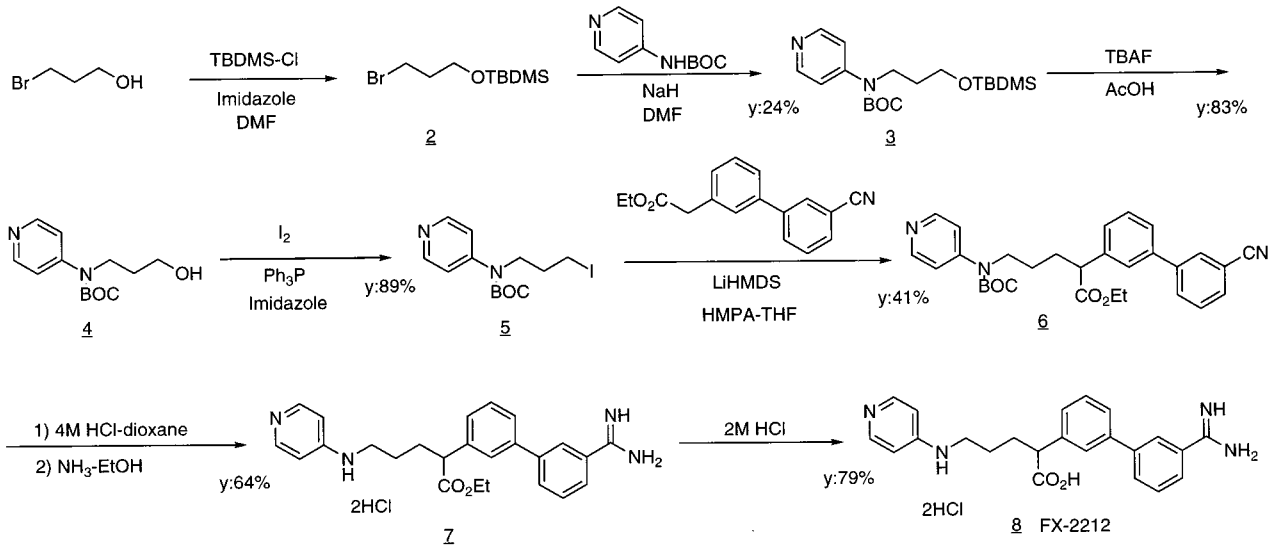

FIG. 2. The scheme of the synthesis of FX-2212. *N-tert*-Butoxycarbonyl-*N*-3-(*tert*-butyldimethylsilyloxy)propyl-4-pyridylamine 3: 2 was prepared from 3-bromo-1-propanol and *tert*-butyldimethylsilyl chloride. To a solution of 4-*tert*-butoxycarbonylaminopyridine (400 mg, 2.1 mmol) in *N*,*N*′-dimethylformamide (DMF) (4 ml) was added 60% NaH (83 mg, 2.1 mmol) and 2 (1.0 g, 4.2 mmol) in DMF (6 ml), and the mixture was stirred for 12 h. After work up and purification, 375 mg of 3 was obtained. *N-tert*-Butoxycarbonyl-*N*-3-hydroxypropyl-4-pyridylamine 4: To a solution of 3 (375 mg, 1.0 mmol) in tetrahydrofuran (THF) (10 ml) was added acetic acid (175 μl, 3.1 mmol) and 1 M tetrabutylammonium fluoride in THF (3.1 ml, 3.1 mmol) at room temperature, and the mixture was stirred for 3 h. After work up and purification, 213 mg of 4 was obtained. *N-tert*-Butoxycarbonyl-*N*-3-iodopropyl-4-pyridylamine 5: 4 (212 mg, 0.84 mmol) in CH_2Cl_2 (6 ml) was treated with triphenylphosphine (550 mg, 2.1 mmol), iodine (426 mg, 1.7 mmol), and imidazole (143 mg, 2.1 mmol) at 0°C for 0.5 h. After work up and purification, 272 mg of 5 was obtained. Ethyl 5-(*N-tert*-butoxycarbonyl-*N*-4-pyridylamino)-2-(3′-cyano-3-biphenylyl)pentanoate 6: After ethyl 3′-cyanophenyl-3-phenylacetate (295 mg, 1.1 mmol) in THF (3 ml) was added dropwise to a mixture of 1 M lithium bis(trimethylsilyl) amide in THF (1.16 ml, 1.2 mmol) and hexamethylphosphoramide (750 μl, 4.3 mmol) in THF (3 ml) and stirred for 0.5 h at −78°C, 5 in THF (4 ml) was added to the mixture, and the reaction mixture was allowed to reach room temperature. After work up and purification, 153 mg of 6 was obtained. Ethyl 2-(3′-amidino-3-biphenylyl)-5-(4-pyridylamino)pentanoate dihydrochloride 7: After treating 6 (40 mg, 0.08 mmol) in ethanol (1 ml) with 4 M HCl–dioxane (10 ml) at room temperature for 2 days, the mixture was concentrated. The residue was dissolved in ethanol (10 ml) and bubbled with NH_3 gas until saturation at 0°C. After stirring at room temperature for 3 days, the reaction mixture was concentrated *in vacuo*. The residue was purified to give 25 mg of 7. FX-2212, 2-(3′-amidino-3-biphenylyl)-5-(4-pyridylamino)pentanoic acid dihydrochloride 8: 7 (20 mg, 0.04 mmol) was dissolved in 2 M HCl (4 ml), and the mixture was refluxed for 2 h. After concentration and purification, 15 mg of FX-2212 was obtained as white solids. The identity of the compound was checked by NMR and MS.

Inhibitor Binding. The racemic mixture of FX-2212 inhibits factor Xa activity by 50% (IC_{50}) at 272 nM but shows very weak inhibition for thrombin activity even at 100 μM (data not shown). Although the racemic mixture was present in the crystallization solutions, only the *S*-isomer of FX-2212 (FX-2212a) binds to factor Xa. The binding of FX-2212a to factor Xa involves three interaction sites (Figs. 1 and 5). The first interaction involves the biphenylamidine group occupying the S1 pocket. The second is between the pyridine ring of FX-2212a and the factor Xa-specific aryl-binding site, which is comprised of Tyr-99, Trp-215, and Phe-174. The third interaction between the carboxyl group of FX-2212a and residues in the catalytic site is mediated through water molecules. In all three crystallographically independent factor Xa molecules, the binding mode of FX-2212a to the factor Xa active site is almost preserved, despite the fact that the crystal packing interactions around the binding site are different.

Table 1. Diffraction data and refinement statistics

	Crystal form 1	Crystal form 2
Resolution, Å	2.4	2.3
Measurements, *n*	78,773	46,925
Unique reflections	26,594	14,542
Data completeness	30–2.4 Å 91.2%	30–2.3 Å 96.2%
	2.53–2.4 Å 58.4%	2.4–2.3 Å 95.2%
R_{sym} on intensity*, %	5.7	8.5
Reflections used in refinement	24,386	14,081
R value†	8.0–2.4 Å 20.6%	8.0–2.3 Å 19.6%
R-free‡, %	29.4	28.7
rms deviation from ideal bond length, Å	0.008	0.007
rms deviation from ideal bond angle, °	1.31	1.24
B value for nonhydrogen protein atoms, Å²	24.1	15.6
rms deviation in *B* value of bonded atoms, Å²	1.74	1.64
Nonhydrogen atoms, *n*	5,433	2,790
Water molecules, *n*	302	211

*$R_{sym} = \Sigma|I(h) - \langle I(h)\rangle|/\Sigma\, I(h)$.

The binding in the S1 site involves the formation of salt bridges between the amidino group of FX-2212a and the carboxyl group of Asp-189 in twin–twin geometry (Fig. 5*b*). The biphenyl ring makes hydrophobic interactions with residues in the S1 pocket. The first phenyl ring, which contains the amidino group, makes hydrophobic interactions with the main chain of Ala-190–Cys-191 and Trp-215–Gly-216. The second phenyl ring, which links the benzamidine group to the pentanoic acid, makes hydrophobic interactions with the side chain of Gln-192. This interaction causes the main chain of Gln-192 to move ≈1.0 Å toward the biphenyl ring.

In the second interaction site, the pyridine ring of FX-2212a is located in the center of the aryl-binding site and parallel to the indole ring of Trp-215. Hydrophobic interactions are made mainly between the pyridine ring of FX-2212a and Trp-215. In

FIG. 3. Ribbon drawing of the Des[1–44] factor Xa-FX-2212a complex structure (only one molecule in the form 1 crystal is shown). The light chain consists of the first (yellow) and the second EGF domains (orange). The trypsin-like catalytic domain is shown in blue. FX-2212a (red ball and stick) is bound to the active site. One calcium ion (pink) each is bound to the first EGF domain and the catalytic domain. The binding region for the effector protease receptor-1 is shown in magenta.

of Ile-175 through a water molecule, "A" (558 and 672 in the crystal form 2, 578 in the crystal form 1). This water, Wat A, also is preserved in the apo factor Xa structure (518 in 1HCG).

The carboxyl acid of the inhibitor is directed toward the catalytic triad and makes interactions with residues in the active site and other residues through water molecules (Figs. 1 and 5*b*). It is clear from the electron density maps that only the *S*-isomer of FX-2212a binds to the factor Xa in all three crystallographically independent molecules (Fig. 5*a*). Although the interactions at the open side of the inhibitor binding pocket are different among the three independent complexes (shown in orange in Fig. 5*b*), the hydrogen bonding network at the covered side of the pocket between FX-2212a and the factor Xa remains the same (shown in green in Fig. 5*b*). The first conserved water molecule, Wat B (790 and 670 in the form 1, 519 in the form 2), mediates the binding between one oxygen of the carboxyl group of FX-2212a and Oη of Tyr-99. Two other conserved water molecules are located in the hydrogen bonding range from Wat B. One is Wat C (789 and 649 in form 1, 520 in form 2), which makes hydrogen bonds to Nε of His-57 and to Nε of Gln-61, and the other is Wat D (791 and 648 in form 1, 518 in form 2), which makes hydrogen bonds to Oγ of Ser-195 and to O of Ser-214. The side chain of the catalytic Ser-195 rotates by $\approx$130° from the position in the apo-factor Xa structure, in which the Oγ of Ser-195 makes a hydrogen bond with Nε of His-57. Also, Wat E (793 and 652 in form 1, 521 in form 1) makes hydrogen bonds to O of Phe-41, N of Gly-193, and Wat C. These conserved water molecules may represent the potential site to introduce modification groups in designing new inhibitors.

DISCUSSION

In contrast to the abundance of crystal structures of complexes between thrombin and chemical inhibitors (33–45), our structure is only the second structure of the inhibitor-bound factor Xa. The structure of the DX-9065a-bound factor Xa was the first inhibitor complex structure published (13). DX-9065a was developed by Daiichi Pharmaceutical Co., Ltd., Tokyo, and inhibits factor Xa with K_i = 41 nM; IC_{50} = 92 nM at pH 8.4 (46, 47) and K_i = 103 nM; IC_{50} = 208 nM at pH 7.4 (data not shown). Although the chemical structure and the binding mode of this inhibitor are different from those of FX-2212a (Fig. 1), neither inhibitors interact directly with the S2 and S3 sites, in contrast to many thrombin inhibitors. Because the S2 site is entirely blocked by the large side chain of Tyr-99, which is consistent with the preference of glycine for the P2 site, the S2 site does not seem to be available for the binding of factor Xa inhibitors. The S3 site, in which the P3 residue of the substrate makes an antiparallel β-ladder with Gly-216, was not involved in inhibitor binding either.

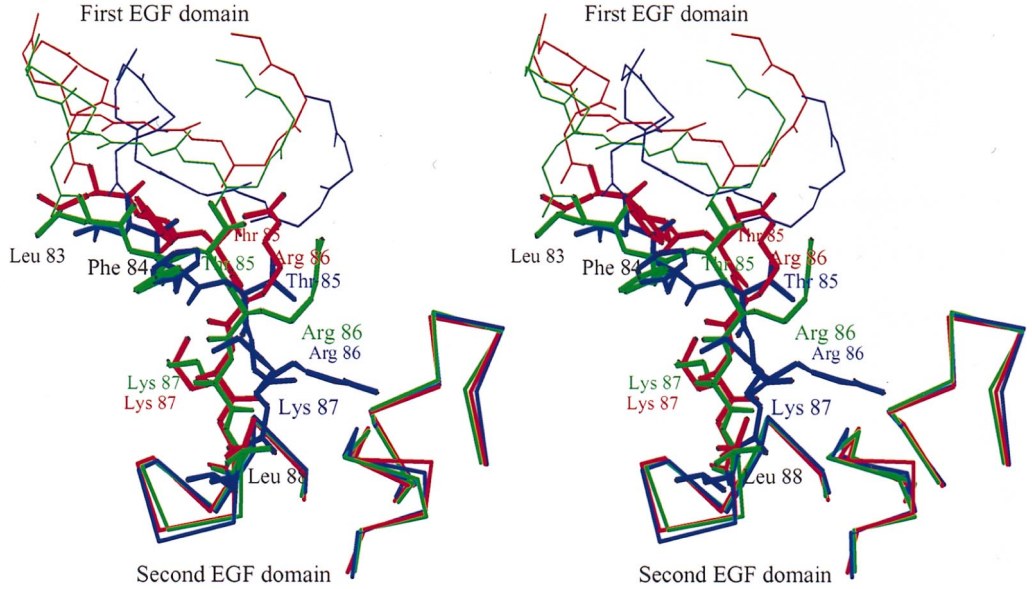

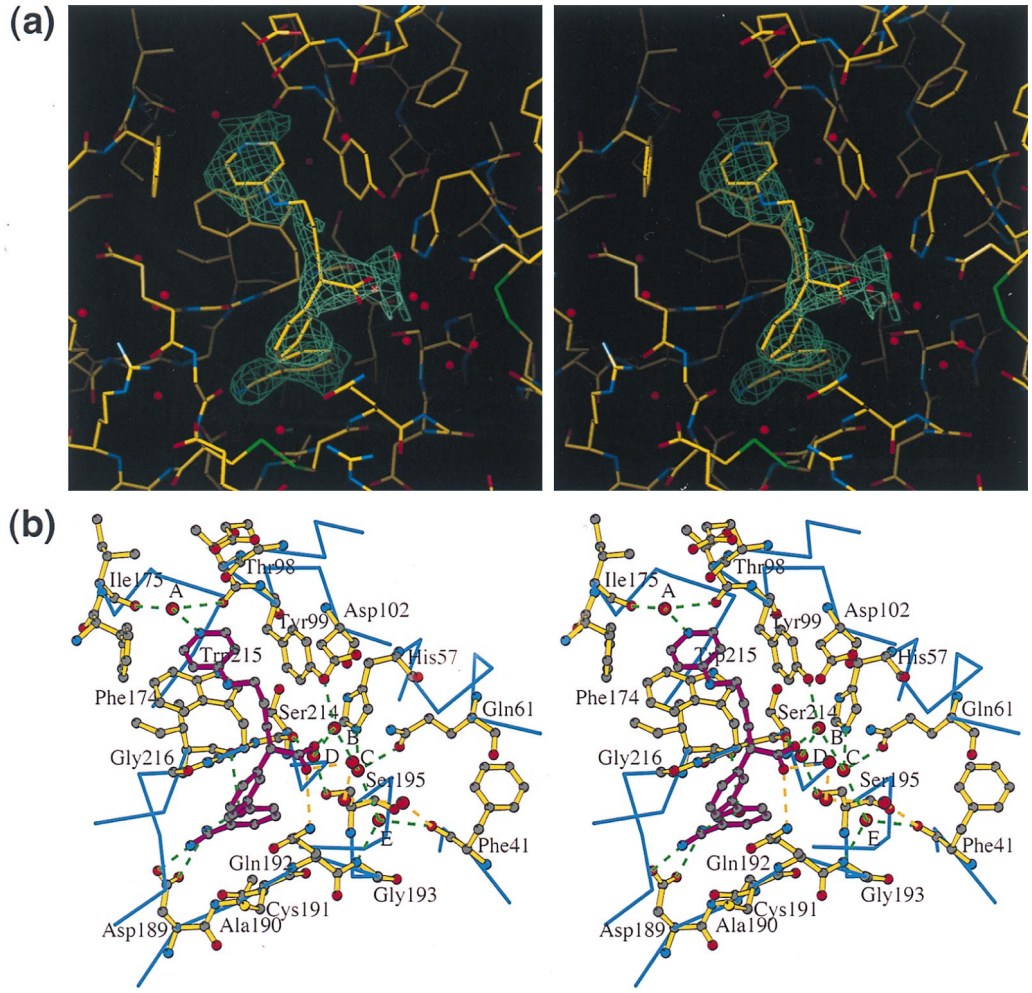

FIG. 5. (*a*) Stereo view of the electron density for FX-2212a in difference electron density maps (contoured at 1.6σ) calculated after modeling the first EGF domain and the simulated annealing refinement. The final structure is superimposed. (*b*) Binding interactions of FX-2212a (magenta ball and stick) with Des[1–44] factor Xa in the form 1 crystal. The Cα backbone is shown in blue, and residues involved in interaction are shown as a yellow ball-and-stick model. Conserved hydrogen bonds in the three crystallographically independent molecules are shown in green and a unique hydrogen bond in this interaction is shown in orange.

The lack of availability of the S2 site may be compensated by the interaction to Gln-192: The second phenyl ring, which links the benzamidine group to the pentanoic acid, makes hydrophobic interactions with the aliphatic portion of the side chain of Gln-192. The rotation around the bond between the two phenyl rings allows the second phenyl ring to be positioned in parallel to the side chain amide group of Gln-192 without breaking the twin–twin geometry interaction between the amidino group and Asp-189. Gln-192, which defines the preference of the P3 site, has moved closer toward the inhibitor than in the apo-factor Xa structure. In the DX-9065a-bound factor Xa structure, Gln-192 also moves and makes hydrophobic interactions with the naphthyl ring, but the more rigid ring structure does not seem to allow the twin–twin geometry interaction between the amidino group and Asp-189 at the same time.

The structure of Des[1–44] factor Xa in complex with the new synthetic inhibitor FX-2212a provides us useful information for directing a search for the next generation of inhibitors with improved properties.

We thank Kyeong-Kyu Kim and Jarmila Jancarik (University of California, Berkeley) for useful suggestions, and Malcolm Capel (NSLS beam line X12B) for help with data collection. This work has been supported by the Director, Office of Energy Research, Office of Basic Energy Sciences, Division of Chemical Sciences of the U.S. Department of Energy (under contract DE-AC03-76SF00098) and Banyu Pharmaceutical Co., Ltd., Tokyo.

1. Davie, E. W., Fujikawa, K. & Kisiel, W. (1991) *Biochemistry* **30,** 10363–10370.
2. Sturzebecher, J. & Meier, J. (1995) *J. Enzyme Inhibition* **9,** 1–2.
3. Tapparelli, C., Metternich, R., Ehrhardt, C. & Cook, N. S. (1993) *Trends Pharmacol. Sci.* **14,** 366–367.
4. Hussain, M. A., Knabb, R., Aungst, B. J. & Ketterner, C. (1991) *Peptides* **12,** 1153–1154.
5. Bajusz, S., Szell, E., Bagdy, D., Barabas, E., Horvath, G., Dioszegi, M., Fittler, Z., Szabo, G., Juhasz, A., Tomori, E., *et al.* (1990) *J. Med. Chem.* **33,** 1729–1735.
6. Freund, M., Cazennave, J. P., Courtney, M., Degryse, E., Roitshc, C., Bernat, A., Delebassee, D., Defreyn, G. & Maffrand, J. P. (1990) *Thromb. Haemostasis* **63,** 187–192.
7. Jackson, C. V., Crowe, G., Frank, J. D., Wilson, H. C., Coddman, W. J., Utterback, B. G., Jakubowshi, J. A. & Smith, G. F. (1992) *J. Pharmacol. Exp. Ther.* **261,** 546–552.
8. Herbert, J. M., Bernat, A., Dol, F., Heraulr, J. P., Crepon, B. & Lormeau, J. C. (1996) *J. Pharmacol. Exp. Ther.* **276,** 1030–1038.
9. Altieri, D. C. (1994) *J. Biol. Chem.* **269,** 3139–3142.
10. Altieri, D. C. (1995) *J. Leukoc. Biol.* **58,** 120–127.
11. Nicholson, A. C., Nachman, R. L., Altieri, D. C., Summers, B. D., Ruf, W., Edgington, T. S. & Hajjar, D. P. (1996) *J. Biol. Chem.* **271,** 28407–28413.

DOCKET ALARM

Explore Litigation Insights

Docket Alarm provides insights to develop a more informed litigation strategy and the peace of mind of knowing you're on top of things.

Real-Time Litigation Alerts

Keep your litigation team up-to-date with **real-time alerts** and advanced team management tools built for the enterprise, all while greatly reducing PACER spend.

Our comprehensive service means we can handle Federal, State, and Administrative courts across the country.

Advanced Docket Research

With over 230 million records, Docket Alarm's cloud-native docket research platform finds what other services can't. Coverage includes Federal, State, plus PTAB, TTAB, ITC and NLRB decisions, all in one place.

Identify arguments that have been successful in the past with full text, pinpoint searching. Link to case law cited within any court document via Fastcase.

Analytics At Your Fingertips

Learn what happened the last time a particular judge, opposing counsel or company faced cases similar to yours.

Advanced out-of-the-box PTAB and TTAB analytics are always at your fingertips.

API

Docket Alarm offers a powerful API (application programming interface) to developers that want to integrate case filings into their apps.

LAW FIRMS
Build custom dashboards for your attorneys and clients with live data direct from the court.

Automate many repetitive legal tasks like conflict checks, document management, and marketing.

FINANCIAL INSTITUTIONS
Litigation and bankruptcy checks for companies and debtors.

E-DISCOVERY AND LEGAL VENDORS
Sync your system to PACER to automate legal marketing.